


# Risk Constrained Energy Efficient Optimal Operation of a Converter Governed AC/DC Hybrid Distribution Network With Distributed Energy Resources and Volt-VAR Controlling Devices

Subho Paul , *Member, IEEE*, Abhimanyu Sharma, and Narayana Prasad Padhy, *Senior Member, IEEE*

**Abstract**—Increasing penetration of direct current (dc) based distributed energy resources and dc loads in the conventional alternating current (ac) network necessitate the deployment of ac/dc hybrid distribution networks (HDNs). In view with the development of advanced energy management policy for ac/dc HDNs, unlike previous literatures, this article proposes a risk constrained energy efficient management algorithm by merging load shifting (LS) and conservation voltage reduction (CVR) techniques. The optimization framework aims to simultaneously minimize both true and conditional risk or conditional value at risk values of the expected energy cost under uncertain solar power generation, load demand, and upper grid energy price. In contrast with the available stochastic optimization process, in this article, two-point estimation strategy is employed in place of Monte Carlo simulation for scenario generation from the probability density functions of the uncertain parameters to reduce computational exertion. The proposed centralized optimization framework is initially developed as mixed integer nonconvex programming but to avoid computation complexity, the nonlinear components are replaced by their linear counterparts. Later, a new solution process named successive mixed integer linear programming (s-MILP) is proposed to obtain the optimal decisions for deployment of LS and CVR through smart inverters and volt-VAR controlling devices. Efficacy of the proposed technique is demonstrated on modified IEEE 33 bus ac/dc HDN and the most energy efficient operation is found by merging LS and CVR. Simulation outcomes prove fast and near optimal convergence of the s-MILP compared to conventional second-order conic programming relaxed mixed integer convex programming and

piecewise linearization based MILP. Further, to assess the impact of network size on the solution time and optimality, the proposed advanced distribution network management systems strategy is employed on 132 bus ac/dc HDN.

**Index Terms**—Alternating current (ac)/direct current (dc) hybrid distribution network (HDN), conditional value at risk (CVaR), conservation voltage reduction (CVR), load shifting (LS), successive mixed integer linear programming (s-MILP), two-point estimation (2PE).

## NOMENCLATURE

### A. Abbreviations, Sets, and Indices

ADNMS	Advanced distribution network management system
(H)DN	(Hybrid) distribution network
LS	Load shifting
CVR	Conservation voltage reduction
CVaR	Conditional value at risk
MI(N)CP	Mixed integer (non)convex programming
MILP	Mixed integer linear programming
MCS	Monte Carlo simulation
pdf	Probability distribution function
SOCP	Second-order conic programming
VVC	Volt-VAR control
(2)PE	(Two) point estimation
VR, CB	Voltage regulator and capacitor bank, respectively
VSC	Voltage source converter
$N$	Set of total number of buses indexed by $n$ , $m$ , and $k$
$N_{AC}, N_{DC}$	Set of total number of ac and dc buses, respectively
$S$	Set of total number of scenarios indexed by $s$
$M, K$	Set of parent and child nodes, respectively
$T$	Total number of time intervals indexed by $t$

### B. Parameters

$P_{n,t}^{L,F}$	Forecasted active power demand in kW
$f(\cdot)$	Probability density function

Manuscript received January 12, 2021; revised April 4, 2021; accepted May 10, 2021. Date of publication May 18, 2021; date of current version July 16, 2021. Paper 2021-IACC-0010.R1, presented at the 2020 IEEE International Conference on Power Electronics, Smart Grid and Renewable Energy, Cochin, India, Jan. 2–4, 2020, and approved for publication in the IEEE TRANSACTIONS ON INDUSTRY APPLICATIONS by the Industrial Automation and Control Committee of the IEEE Industry Applications Society. This work was supported in part by the Department of Science and Technology, India Smart Grid Research initiatives under the Research Grant U.S.–India Collaborative for Smart Distribution System with Storage (UI-ASSIST: IUS-1132-EED); in part by the Indo–U.K. Collaboration for Zero Peak Energy Building Design for India (ZED-I: DST-1161-APD); in part by the Demonstration of MW-Scale Solar Integration in Weak Grids Using Distributed Energy Storage Architecture (D-SIDES:DST-1237 EED); and in part by the Indo–Danish collaboration for data-driven control and optimization for a highly Efficient Distribution Grid (ID-EDGE). (Corresponding author: Subho Paul.)

The authors are with the Department of Electrical Engineering, Indian Institute of Technology Roorkee, Roorkee 247667, India (e-mail: spaul@ee.iitr.ac.in; abhimanyu1@ee.iitr.ac.in; nppadhy@ee.iitr.ac.in).

Color versions of one or more figures in this article are available at <https://doi.org/10.1109/TIA.2021.3081526>.

Digital Object Identifier 10.1109/TIA.2021.3081526

$\mu_{n,t}^{L,F}, \sigma_{n,t}^{L,F}$	Mean and standard deviation (SD) of pdf related to load uncertainty, respectively	<i>C. Decision Variables</i>	
$p f_n$	Power factor	$P_{s,n,t}^L$	Actual active power demand in kW
$P_{s,n}^{\text{sh,max}}$	Maximum available shiftable demand in kW	$P_{s,n,t}^{\text{sh}}$	Amount of shifted active power demand in kW
$Z_{P/Q}, I_{P/Q}, P_{P/Q}$	Constant impedance, current, and power coefficients of active/reactive power demand	$Q_{s,n,t}^L$	Actual reactive power demand in kVAR
$V_{\text{min/max/nom}}^{\text{ac}}$	Minimum, maximum, and nominal values of ac bus voltage, respectively, in kV	$P_{s,n,t}^{L,\text{cwr}}$	ZIP model of active power demand in kW
$V_{\text{min/max/nom}}^{\text{dc}}$	Minimum, maximum, and nominal values of dc bus voltage, respectively, in kV	$Q_{s,n,t}^{L,\text{cwr}}$	ZIP model of reactive power demand in kVAR
$P_{n,t}^{\text{PV}}$	Forecasted active power generation from solar panel in kW	$Q_{s,n,t}^{\text{PV}}$	Reactive power injection from solar inverter in kVAR
$\eta_{\text{PV}}$	Efficiency of solar panel	$E_{s,n,t}^{\text{bat}}$	Energy level of battery storage in kWh
$A_n^{\text{PV}}$	Area of solar panel in m <sup>2</sup>	$P_{s,n,t}^{\text{bat, ch/dch}}$	Charging/discharging power of battery storage in kW
$Irr_t$	Solar irradiation in kW/m <sup>2</sup>	$\lambda_{n,t}^{\text{bat, ch/dch}}$	Charging/discharging status of battery, 1-Yes, 0-No
$T_{\text{amb}}$	Outdoor temperature in °C	$Q_{s,n,t}^{\text{bat}}$	Reactive power injection from battery inverter in kVAR
$\bar{P}_n^{\text{PV}}$	Solar panel capacity in kW	$V_{s,n,t}$	Bus voltage magnitude in kV
$\mu_{n,t}^{\text{PV}}, \sigma_{n,t}^{\text{PV}}$	Mean and SD of pdf related to solar power generation uncertainty, respectively	$T_{n,t}^{\text{VR}}$	Tap position of VR
$\bar{S}_n^{\text{PV}}$	Rating of the solar inverter in kVA	$Q_{s,n,t}^{\text{CB}}$	Reactive power supply from CB in kVAR
$\eta_{\text{bat}}$	Battery efficiency	$SW_{n,t}^{\text{CB}}$	Switching status of CB, 1-ON, 0-OFF
$\Delta t$	Gap between two time intervals in hour	$P_{s,mn,t}^{\text{flow, ac/dc}}$	Power flow in ac/dc lines in kW
$\bar{P}_n^{\text{bat}}$	Power rating of battery in kW	$I_{s,mn,t}^{\text{ac/dc}}$	Current flow in ac/dc lines in kA
$E_{n,\text{min/max}}^{\text{bat}}$	Minimum and maximum allowable energy level of battery storage, respectively, in kWh	$Q_{s,mn,t}^{\text{flow, ac}}$	Reactive power flow in ac lines in kVAR
$\bar{S}_n^{\text{bat}}$	Rating of the battery inverter in kVA	$P_{s,n,t}^{\text{VSC, ac}}$	Active power injection from ac side of VSC station in kW
$\Delta V_n$	Change in voltage magnitude for every change in tap position of VR	$Q_{s,n,t}^{\text{VSC, ac}}$	Reactive power injection from ac side of VSC station in kVAR
$T_{n,\text{min/max}}^{\text{VR}}$	Minimum and maximum tap position of VR	$P_{s,n,t}^{\text{VSC, dc}}$	Active power injection from dc side of VSC station in kW
$NT_n^{\text{VR}}$	Maximum allowable tap operations in the time period of VR	$V_{s,n,t}^{\text{VSC, ac/dc}}$	AC/dc side voltage of VSC station in kV
$\bar{Q}_n^{\text{CB}}$	Rating of CB in kVAR	$M_{s,n,t}$	Modulation index (MI) of VSC
$NS_n^{\text{CB}}$	Maximum allowable switching operations in the time period of CB	$P_{s,n,t}^{\text{VSC, loss}}$	Active power loss in VSC in kW
$r_{mn}^{\text{ac/dc}}$	AC/dc line resistance in kΩ	$P_{s,t}^{\text{buy/sell}}$	Active power purchase (sell) from (to) upper grid in kW
$x_{mn}^{\text{ac}}$	AC line reactance in kΩ	$Q_{s,t}^{\text{buy}}$	Reactive power grabbed from upper grid in kVAR
$\nu^{\text{VSC}}$	Loss coefficient of VSC	$\lambda_t^{\text{buy}}$	Status of grid power purchase, 1-Yes, 0-No
$\eta^{\text{VSC}}$	Efficiency of VSC		
$\bar{S}_n^{\text{VSC}}$	Rating of VSC in kVA		
$\bar{S}_{mn}^{\text{flow}}$	Thermal capacity of lines in kVA		
$P^{\text{max}}$	Maximum main grid feeder capacity in kW		
$r_{s,t}^{\text{buy}}$	Day ahead upper grid energy purchase price in Rs./kWh		
$\varphi$	Percentage value of energy purchase price for setting energy sell price in Rs./kWh		
$\rho_s^{\text{PV}}, \rho_s^{L,F}, \rho_s^{\text{buy}}$	Probability of each scenario for solar power generation, load, and energy purchase price, respectively		
$\mu_t^{\text{buy}}, \sigma_t^{\text{buy}}$	Mean and SD of pdf related to energy purchase price uncertainty, respectively		
$\gamma$	Risk aversion parameter		

## I. INTRODUCTION

### A. Background and Motivation

IN THE era of 19th century, the war between Thomas Edison and Nikola Tesla ended with the win of alternating current (ac) system due to numerous advantages of ac at that time period [1]. This reformed the power sector, from generation to transmission and distribution, as an ac network. Since the last few decades, urbanization, industrial revolution, and population growth enhanced the energy requirement in all over the world. International Energy Agency showed in 2017 that the energy requirement of the entire world was increased by 30% during 2007 to 2017 (18231 TWh to 23696 TWh) [2]. These lead to over

exploitation of the fossil fuels by the power generation companies which creates global warming threat. A generic distribution network operator (DNO) mainly aims to meet its customer's satisfaction. Therefore, this unavoidable excess demand requires new power plant installation, which will breach the directives of Paris agreement [3]. To reduce environmental hazards, green energy resources are penetrating into the power sector especially as solar power, generated from the photovoltaic (PV) panels as direct current (dc) power. Again, the intermittency present in the solar power is mitigated by the battery storages, which is also a dc equipment. Generally, the dc distributed energy resources (DERs) like solar panels and batteries are integrated with the conventional ac DNs through smart inverters to keep the overall network architecture as ac type. Recent advancement in the dc power electronics loads (like dc computer, electric vehicles, LED lights, etc.) bring back the dc system in the power sector to reduce the conversion loss. However, existing ac systems cannot be obsoleted completely. Therefore, to incorporate the advantageous attributes of the dc network with the benefits of conventional ac networks, concept of ac/dc hybrid distribution network (HDN) is gaining popularity [4].

In present time, advanced distribution network management systems (ADNMS) are designed for peak load reduction and maximum utilization of the green energies with the help of different load reduction processes viz. load shifting (LS) and conservation voltage reduction (CVR) while preserving both system security and customers' satisfaction [5]. However, design of an ADNMS strategy for any DN is quite cumbersome job as the developed optimization portfolio takes the form of a mixed integer nonconvex programming (MINCP) due to introduction of both continuous and discrete variables in the nonconvex optimal power flow model. Previously, many researches were carried out to design complex MINCP-based ADNMS for ac DN [6], [7], [8]. This becomes further laborious to design and solve if DNs have power electronics converters, i.e., for ac/dc HDNs. Generally, day ahead strategies are developed as simple deterministic one by considering the forecasted data regarding solar power generation, load demand, and upper grid energy price as error free. Present forecasting processes utilizing regression analysis [9], machine learning [10], etc. are quite trustworthy in current scenarios. However, abrupt change in weather conditions, uncertain lifestyle of the users, and power system deregulation will make the forecasting process complex in next few decades [11]. Therefore, the economic risk associated with the DN management due to forecasting error needs to be evaluated properly.

Aiming toward building a new ADNMS for ac/dc HDNs, this article elucidates a risk constrained day ahead energy efficient DN management portfolio for ac/dc HDNs consisting of DER with smart inverters, VSC stations, and VVC devices.

## B. Literature Review

Initially, ac/dc systems are deployed at single microgrid structure to check its feasibility and advantages over only ac systems [11], [12]. However, presently various research works are going on for successful deployment of ac/dc system in distribution

networks. Murari *et al.* [13], [14] proposed graph theory based load flow solution process for ac/dc DNs by utilizing the concept of linear algebra. Tylavsky *et al.* [15] implemented Newton–Raphson load flow strategy to ac/dc systems. Ahmed *et al.* [16] developed unified power flow model by modeling different power electronics converters. The economic impact of the ac/dc network configuration on the DN usage charge was assessed in [17].

The above literatures [13]–[17] focus only to determine the power flow solution and do not aim to optimize the operation of ac/dc HDN resources. For proper planning of ac/dc HDN, a genetic algorithm (GA) based approach was designed in [18] considering only critical loads. The planning problem was designed as a two-level nested problem, where upper level determined the configuration of the network and the lower level solved the optimal power flow problem. Another GA-based deterministic planning problem was portrayed in [19] for ac/dc HDN to determine the optimal location and size of the substations, length, and capacity of the cables, and routing of ac and dc feeders. Technoeconomic benefits of ac/dc HDN over only ac DN was explored by [20]. The MINCP-based two-stage economic dispatch problem was solved using nondominated sorting genetic algorithm (NSGA-II) associated with interior point method to maintain system security and reliability. Optimal configuration of urban ac/dc network was investigated in [21] by converting some existing ac lines to dc lines. A chance constrained bilevel stochastic problem was proposed where in upper level the network configuration was determined and its optimal day ahead operation with newly installed VSCs was scheduled in the lower level. The problem was formed as MINCP and solved using NSGA-II.

In order to design energy management topology, Qi *et al.* [22] developed a deterministic MINCP-based optimization process for successful interaction between ac DN and one dc microgrid, connected through VSC. Authors propounded a decentralized iterative solution process to secure economic operation of the grids with critical loads when working in individual or collaborative manner. Baboli *et al.* [23] designed a stochastic energy management system for ac/dc microgrid considering uncertain renewable power, load, and energy price. Eajal *et al.* [24] proposed a bilevel MINCP-based centralized stochastic framework for optimal dispatch of two lumped ac and dc grids connected through a bidirectional ac–dc converter. The dispatch problem considered uncertainty in renewable generation, critical load profile, and market energy price. Fu *et al.* [25] proposed a Stackelberg game based bilevel robust optimization framework for energy management in ac/dc HDN considering renewable generation uncertainty. The problem was formulated as MICP by adopting SOCP relaxed model of the DN. Ahmed *et al.* [26] proposed a deterministic day ahead energy management portfolio for ac/dc HDN considering network reconfiguration. The problem was framed as MILP after linearizing the nonconvex DN models using certain assumptions. A distributed optimization framework was propounded by [27] considering uncertain wind power, modeled by 1-norm and  $\infty$ -norm based data-driven techniques. Polyhedral linearization method was adopted to represent the quadratic expressions as a set of linear

expressions. The overall distributed algorithm was solved using alternating direction method of multipliers (ADMM) algorithm. Another ADMM-based distributed optimization framework was proposed by [28] for networked ac/dc microgrids. The problem was formed as robust optimization where unlike stochastic techniques, the uncertain critical load and renewable generations were modeled as zero mean uncertainty set by knowing their range of variation. Qiao and Ma [29] investigated the operation of the VVC devices in ac/dc HDN. However, they modeled the bus demand as constant power loads and formulated the problem as deterministic MINCP to maximize the contribution of the VVC devices to maintain voltage quality. The developed problem was solved using decomposition-based evolutionary algorithm. Power management model for controlling operation of VVC devices in ac/dc HDN was illustrated in [30]. The problem was designed as a mixed integer quadratic constraint programming based Stackelberg noncooperative game between microgrid operators and DNO. Same as [29], in this article, also the loads were modeled as constant power and hence the benefits of CVR were not explored.

The above literatures [18]–[29] did not consider the load management in their study and designed their topology to study the network operation with constant power critical loads. To leverage the benefit of active power demand management, Lotfi and Khodaei [31] added load shedding operation in their ac/dc microgrid planning problem. The optimization problem aimed to minimize the total planning cost and it was designed as MILP. Geng *et al.* [32] proposed a new ac/dc HDN architecture consisting of “multiple park integrated energy subnetwork” and multiport power electronic transformers. The energy management process of the newly proposed network was developed as a stochastic MINCP considering flexibility provided by the loads, different generating units, and DERs. The uncertain wind generation was modeled as normal pdf and the entire problem was solved using GA.

### C. Research Gaps

It is noticed from above literature survey that ac/dc HDNs consisting of VSCs are gaining research interest in recent time. Though the existing literatures tried to develop secure and reliable energy management strategies for ac/dc HDNs but still the following research gaps can be identified:

- 1) The energy management problems are mainly designed considering the loads as critical in nature [18]–[29]. Only [32] adopted load flexibility to design their technique. Literatures [29] and [30] developed their model with VVC devices but had not deployed CVR. Therefore, the available ac/dc HDN management systems are not advanced and need further refinement.
- 2) Deterministic energy management systems [22], [26], [29], [31] lack from the flexibility of handling uncertain conditions. Stochastic frameworks [23], [24], [27], [32] resolve this issue by including the possible scenarios in the decision-making process by minimizing the expected cost. However, it cannot give proper insight about the financial risks associated with the uncertain solar power

generation, load demand, and upper grid energy price. Risk-constrained optimization portfolio is challenging to design if it is merged with the nonconvex ac/dc network model. As per the authors’ knowledge, there is no such study which elaborates the risk constrained ac/dc HDN management with VSCs, smart inverter collocated DERs, and VVC devices.

- 3) Number of decision variables and constraints for stochastic and risk-constrained optimization frameworks increase exponentially with the number of generated scenarios from the estimated pdfs of the uncertain parameters [23], [24], [27], [32]. Conventionally, MCS followed by scenario reduction technique is adopted for obtaining accurate optimal decisions in expense of huge computational burden and large solution time. Therefore, risk-constrained strategies need advancement for computation time reduction without compromising much with accuracy.
- 4) Energy management techniques are mostly designed as MINCP [18]–[32] due to the nonconvex ac/dc DN model. However, MINCP lacks from efficient solution process and suffers from slow convergence and computation tractability issues. Heuristic solution techniques are adopted in [18]–[21], [29], [32] for solving MINCP, but those suffer from the chance of local convergence. For avoiding convergence issues, some literatures, [25], [30], adopted SOCP relaxations in the HDN model to simplify the optimization problem as MICP, which is efficiently solved by several decomposition strategies. However, decomposition strategies take much larger time to converge as it solves convex optimization at each iteration. Fast convergence feature makes MILP process adaptable to some literatures [11], [12], [26], [27], and [31]. However, they have either neglected the network architecture by considering only a simple microgrid [11], [12], [31] or adopted some assumptions [26]. Piecewise and polyhedral linearizations are adopted in [26] and [27], respectively, but the accuracy of the method highly depends on the number of linear segments and more segment causes slow convergence too.

In view with the abovementioned research gaps, authors have proposed a deterministic centralized MILP-based ADNMS portfolio for optimal operation of ac/dc HDN consisting of DERs with smart inverters by leveraging the benefits of only LS in [33]. The simulation results conveyed that LS process succeeded to reduce the peak demand of the HDN by 4.2%. Though the optimization portfolio is developed as MILP, but exclusion of network loss from the energy management process made the study simple. Further, benefit of CVR deployment along with LS for energy efficient operation of the ac/dc HDN, and risk associated with the uncertain solar generation, load demand, and upper grid energy price are still left unexplored.

### D. Research Contributions and Organizations

Design of ADNMS for ac networks are quite popular and explored much in the literatures. Singh and Singh [34] proposed an energy saving methodology by deploying CVR in association

with PV inverters. Shi *et al.* [35] performed LS for peak load reduction. However, CVR and LS were implemented separately in [34] and [35], respectively, and the energy management portfolio was designed as deterministic optimization without considering uncertainties. Hossan *et al.* [36] merged both LS and CVR as stochastic optimization problem for energy efficient operation of DN. However, [34]–[36] have focused to develop risk averse strategy only for ac networks, not having VSCs. Therefore, knowledge regarding risk associated with the uncertainties cannot be obtained from the above literatures. Considering the ADNMS definition given in [5], this article merges peak reduction with the help of LS and CVR to design a risk constrained energy efficient ADNMS for ac/dc HDNs consisting of VSCs, DERs with smart inverters, and VVC devices. As per the authors' knowledge, this is the first study where the above issues are addressed in one literature for designing ac/dc HDN management system. The optimization framework is developed to minimize both expected and conditional value at risk (CVaR) values of the energy cost under uncertain solar generation, load demand, and upper grid energy price. Large computation time is overcome by utilizing two-point estimation (2PE) method in place of conventional MCS-based scenario generation process. Initially, the problem is framed as an MINCP but for fast convergence a successive MILP solution approach is proposed after replacing the nonlinear expressions with their linear counterparts. Distributed optimization approaches were presented in literatures [37] and [38] for optimizing the volt/VAR control and electric vehicle charging operations in ac distribution networks, respectively, using ADMM. Authors had shown the effectiveness of the distributed optimization for handling large distribution networks. However, distributed optimization has several issues in convergence due to its nonconvex nature. Further, the performance (convergence speed) varies with the choice of area partitioning and in the available literatures there is no certain set of specified rules for the same. Real-time deployment of distributed optimization is also complex as it needs several local controllers for proper coordination. In view with the implementation complexity and lack of convergence guarantee for distributed optimization processes, this article presented an efficient centralized risk constrained and fast converging optimization process for obtaining synergistic source-load-storage-VVC device dispatch schedule while satisfying all security and reliability constraints of LS and CVR implementation. The specific contributions are as follows:

- 1) Problem Formulation: An energy efficient ac/dc HDN management system is proposed considering all operational and safety constraints of LS, VVC devices, and smart inverters to leverage the benefit of both LS and CVR deployment. The problem is developed as a joint uncertainty optimization framework after modeling the uncertain solar generation as Beta distribution and uncertain load demand and energy purchase price as Normal distribution around their forecasted mean value. The derived problem aims simultaneous minimization of both true and CVaR values of the expected energy cost.
- 2) Computation: Computation burden and long convergence time due to large number of scenarios are avoided by

replacing MCS followed by scenario reduction methods with 2PE method for scenario generation from the pdfs.

- 3) Solution Process: For reliable and fast convergence of the proposed risk constrained ADNMS framework, different nonconvex expressions are replaced by their linear counterparts. Quadratic expressions in the ac/dc HDN model are approximated by their first-order Taylor series expansion and then the solution process is proposed as a successive mixed integer linear programming algorithm (s-MILP).
- 4) Demonstration and Validation: The efficacy of the proposed ADNMS is demonstrated on modified IEEE 33 bus ac/dc HDN at different operating situations. Computation burden relaxation due to application of 2PE is validated by solving the proposed approach with MCS followed by scenario reduction techniques. Further, effectiveness of s-MILP is checked in terms of computation time and accuracy after comparing with SOCP relaxed MICP and piecewise linearized MILP problems. Investigation on 132 bus ac/dc HDN proves scalability of the proposed technique by producing optimal results within 5 h.

Rest of the article is organized as follows: Section II describes the risk-constrained optimization portfolio for ac/dc HDN with necessary objective function and constraints. Section III illustrates the required linearization strategies and successive MILP solution approach. Case studies on modified IEEE 33 bus and 132 bus ac/dc HDN are demonstrated in Section IV with necessary discussions. Finally Section V concludes the article.

## II. RISK-CONSTRAINED OPTIMIZATION PORTFOLIO

### A. Bus Load Model

Load model is essential part for efficient and economic operation of the DNs. Proper modeling of the active and reactive power demand helps to shift the flexible load from peak price hours to off-peak price hours to avoid the chance of high energy cost. In this article, the uncertainty in forecasted bus active power demand at each time step is considered as Normal pdf as follows:

$$f\left(P_{n,t}^{L,F}\right) = \frac{1}{\sigma_{n,t}^{L,F} \sqrt{2\pi}} \exp\left(-\frac{1}{2}\left(\frac{P_{n,t}^{L,F} - \mu_{n,t}^{L,F}}{\sigma_{n,t}^{L,F}}\right)^2\right) \quad (1)$$

Therefore, the LS constraints are given by

$$P_{s,n,t}^L = P_{s,n,t}^{L,F} - P_{s,n,t}^{\text{sh}} \text{ and } Q_{s,n,t}^L = P_{s,n,t}^L \sqrt{(1/pf_n^2) - 1} \quad (2)$$

$$P_{s,n,t}^{\text{sh}} \leq P_{s,n}^{\text{sh,max}} \quad (3)$$

$$\sum_{t \in T} P_{s,n,t}^{\text{sh}} = 0, \forall s \in S \quad (4)$$

Equation (2) determines the active (for both ac and dc buses) and reactive (only for ac buses) power demand at each node for each scenario. Equation (3) defines that total amount of LS from/to a particular time instant should be upper bounded. To

avoid load curtailment total LS should be zero over the time period as represented in (4).

Deployment of CVR is carried out after properly planning the LS operation. CVR is applied after modeling the active and reactive power demands as quadratic ZIP voltage dependent loads [36], expressed in (5) and (6), respectively:

$$P_{s,n,t}^{L,cvr} = P_{s,n,t}^L (Z_P w_{s,n,t} + I_P u_{s,n,t} + P_P) \quad (5)$$

$$Q_{s,n,t}^{L,cvr} = Q_{s,n,t}^L (Z_Q w_{s,n,t} + I_Q u_{s,n,t} + P_Q) \quad (6)$$

Such that,  $Z_P + I_P + P_P = Z_Q + I_Q + P_Q = 1$  and

$$(V_{n,\min}/V_{n,\text{nom}})^2 \leq w_{s,n,t} \leq (V_{n,\max}/V_{n,\text{nom}})^2, \forall s, n, t \quad (7)$$

$$(V_{n,\min}/V_{n,\text{nom}}) \leq u_{s,n,t} \leq (V_{n,\max}/V_{n,\text{nom}}), \forall s, n, t \quad (8)$$

where

$$V_{n,\min/\max/\text{nom}} = \begin{cases} V_{\min/\max/\text{nom}}^{AC}, n \in N_{ac} \\ V_{\min/\max/\text{nom}}^{DC}, n \in N_{dc} \end{cases} \quad (9)$$

### B. Model of Smart Inverter Associated DERs

In this article, only solar generation and battery storage devices are considered as DERs. Though both are dc power sources, but in the study it is considered that they can be connected to both ac and dc buses. For dc buses, they are directly connected, whereas a smart inverter is employed to connect them with the ac buses. Forecasted maximum active power output from solar panels at bus  $n$  at time  $t$  is given by [11]

$$P_{n,t}^{PV} = \eta_{PV} A_n^{PV} Irr_t (1 - 0.005 (T_t^{\text{amb}} - 25)) \quad (10)$$

This forecasted power generation is subjected under uncertainty due to various intermittent environmental factors. Therefore, in this article, solar generation uncertainty at each time step is modeled as Beta probability distribution as follows [11]:

$$f(P_{n,t}^{PV}) = \frac{\Gamma(a+b)}{\Gamma(a)\Gamma(b)} \left(\frac{P_{n,t}^{PV}}{P_{n,t}^{PV,\max}}\right)^{a-1} \left(1 - \frac{P_{n,t}^{PV}}{P_{n,t}^{PV,\max}}\right)^{b-1} \quad (11)$$

$$a = \left(\frac{1 - \mu_{n,t}^{PV}}{(\sigma_{n,t}^{PV})^2} - \frac{1}{\mu_{n,t}^{PV}}\right) (\mu_{n,t}^{PV})^2, b = a \left(\frac{1}{\mu_{n,t}^{PV}} - 1\right)$$

Here,  $\Gamma(\cdot)$  is gamma function. Now, if the solar panel is connected with ac buses, then reactive power can also be generated from the solar inverters by following the constraint (12):

$$Q_{s,n,t}^{PV} \leq \sqrt{(\bar{S}_n^{PV})^2 - (P_{s,n,t}^{PV})^2} \quad (12)$$

Battery storages are considered to be variable energy supplier and load depending on the available solar energy, load demand, and energy price. Energy level of the battery unit updates by following (13). Active power and stored energy limits of the battery unit are denoted in (14). Constraint (15) prohibits simultaneous charging and discharging operations. To make each following day independent from the previous days, constraint (16) is implemented. Now, same as the solar panel if the battery unit is installed at ac buses then the limits on the available apparent power are limited as per (17):

$$E_{s,n,t}^{\text{bat}} = E_{s,n,t-1}^{\text{bat}} + \left(\eta_{\text{bat}} P_{s,n,t-1}^{\text{bat, ch}} - \left(P_{s,n,t-1}^{\text{bat, dch}} / \eta_{\text{bat}}\right)\right) \Delta t \quad (13)$$

$$0 \leq P_{s,n,t}^{\text{bat, ch/dch}} \leq \lambda_{n,t}^{\text{bat, ch/dch}} \bar{P}_n^{\text{bat}} \text{ and } E_{n,\min}^{\text{bat}} \leq E_{s,n,t}^{\text{bat}} \leq E_{n,\max}^{\text{bat}} \quad (14)$$

$$\lambda_{n,t}^{\text{bat, ch}} + \lambda_{n,t}^{\text{bat, dch}} \leq 1 \quad (15)$$

$$\sum_{t \in T} \left(\eta_{\text{bat}} P_{s,n,t}^{\text{bat, ch}} - \left(P_{s,n,t}^{\text{bat, dch}} / \eta_{\text{bat}}\right)\right) = 0 \quad (16)$$

$$\left(P_{s,n,t}^{\text{bat, ch/dch}}\right)^2 + \left(Q_{s,n,t}^{\text{bat}}\right)^2 \leq \left(\bar{S}_n^{\text{bat}}\right)^2 \quad (17)$$

### C. Model of VVC Devices

For trading-off between CVR deployment and voltage security issues, the VVC devices are operated. Performance of voltage regulators (VRs) are done by setting appropriate tap position according to (18), if the VR is connected between two buses  $n$  (upstream bus) and  $k$  (downstream bus):

$$V_{s,k,t} = V_{s,n,t} + T_{n,t}^{\text{VR}} (\Delta V_n / 100) V_{\text{nom}} \quad (18)$$

Subject to

$$T_{n,\min}^{\text{VR}} \leq T_{n,t}^{\text{VR}} \leq T_{n,\max}^{\text{VR}} \text{ and } V_{n,\min} \leq V_{s,k,t} \leq V_{n,\max} \quad (19)$$

However, multiple time tap operation reduces VR life and increases the maintenance cost. Therefore, to avoid increment in the maintenance and replacement cost of the VR due to frequent tap changing operations, total tap operation over the day are restricted by inequality (20):

$$\sum_{t \in T} |T_{n,t}^{\text{VR}} - T_{n,t-1}^{\text{VR}}| \leq N T_n^{\text{VR}}. \quad (20)$$

Capacitor banks (CBs) are mainly installed for reactive power compensation in the network. In real life, capacitors are switched in and out to preserve the reactive power balance in the network. Thus, reactive power supplied from a CB is given by

$$Q_{s,n,t}^{\text{CB}} = SW_{n,t}^{\text{CB}} \bar{Q}_n^{\text{CB}} v_{s,n,t}, v_{s,n,t} \triangleq V_{s,n,t}^2 \quad (21)$$

Same as VR, frequent switching of the CB is avoided by constraint (22) to increase its life:

$$\sum_{t \in T} |SW_{n,t}^{\text{CB}} - SW_{n,t-1}^{\text{CB}}| \leq N S_n^{\text{CB}} \quad (22)$$

### D. AC/DC Hybrid Distribution Network Model

The entire ac/dc HDN is segregated into three major areas according to their components viz. AC network, dc network, and VSC station as shown in Fig. 1. The following constraints (23)–(41) are designed for the HDN considering the above three areas:

$$P_{s,n,t}^{L,\text{net,ac}} = \sum_{m \in M} \left(P_{s,mn,t}^{\text{flow,ac}} - r_{mn}^{\text{ac}} l_{s,mn,t}^{\text{ac}}\right) - \sum_{k \in K} P_{s,nk,t}^{\text{flow,ac}}, \forall s, t, n \in N_{ac} \quad (23)$$

$$Q_{s,n,t}^{L,\text{net,ac}} = \sum_{m \in M} \left(Q_{s,mn,t}^{\text{flow,ac}} - x_{mn}^{\text{ac}} l_{s,mn,t}^{\text{ac}}\right)$$

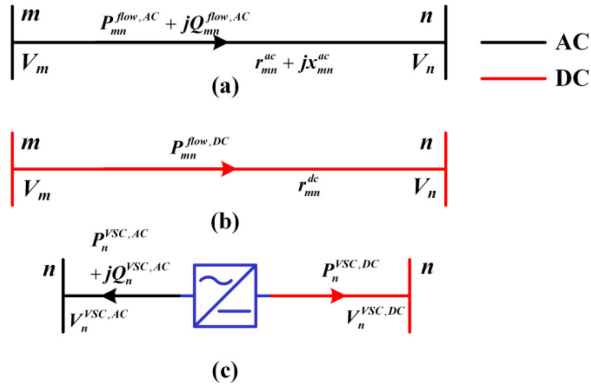


Fig. 1. Different networks in ac/dc HDN. (a) AC network. (b) DC network. (c) VSC station.

$$- \sum_{k \in K} Q_{s,nk,t}^{\text{flow,ac}}, \forall s, t, n \in N_{\text{ac}} \quad (24)$$

$$P_{s,n,t}^{L,\text{net,dc}} = \sum_{m \in M} \left( P_{s,mn,t}^{\text{flow,dc}} - r_{mn}^{\text{dc}} I_{s,mn,t}^{\text{dc}} \right) - \sum_{k \in K} P_{s,nk,t}^{\text{flow,dc}}, \forall s, t, n \in N_{\text{dc}} \quad (25)$$

$$v_{s,n,t} = v_{s,m,t} - 2 \left[ \begin{array}{c} r_{mn}^{\text{ac}} P_{s,mn,t}^{\text{flow,ac}} \\ + x_{mn}^{\text{ac}} Q_{s,mn,t}^{\text{flow,ac}} \end{array} \right] + \left( \frac{(r_{mn}^{\text{ac}})^2}{+(x_{mn}^{\text{ac}})^2} \right) I_{s,mn,t}^{\text{ac}}, \forall m, n \in N_{\text{ac}} \quad (26)$$

$$v_{s,n,t} = v_{s,m,t} - 2r_{mn}^{\text{dc}} P_{s,mn,t}^{\text{flow,dc}} + (r_{mn}^{\text{dc}})^2 I_{s,mn,t}^{\text{dc}}, \forall m, n \in N_{\text{dc}} \quad (27)$$

$$P_{s,n,t}^{L,\text{net,ac}} = P_{s,n,t}^{L,\text{cvr}} - P_{s,n,t}^{\text{PV}} + P_{s,n,t}^{\text{bat,ch}} - P_{s,n,t}^{\text{bat,dch}} - P_{s,n,t}^{\text{VSC,ac}} \quad (28)$$

$$Q_{s,n,t}^{L,\text{net,ac}} = Q_{s,n,t}^{L,\text{cvr}} - Q_{s,n,t}^{\text{PV}} - Q_{s,n,t}^{\text{bat}} - Q_{s,n,t}^{\text{CB}} - Q_{s,n,t}^{\text{VSC,ac}} \quad (29)$$

$$P_{s,n,t}^{L,\text{net,ac}} = P_{s,n,t}^{L,\text{cvr}} - P_{s,n,t}^{\text{PV}} + P_{s,n,t}^{\text{bat,ch}} - P_{s,n,t}^{\text{bat,dch}} - P_{s,n,t}^{\text{VSC,dc}} \quad (30)$$

$$(V_{n,\text{min}})^2 \leq v_{s,n,t} \leq (V_{n,\text{max}})^2, \forall n \in [N_{\text{ac}}, N_{\text{dc}}] \quad (31)$$

$$I_{s,mn,t}^{\text{ac}} = \left( \left( P_{s,mn,t}^{\text{flow,ac}} \right)^2 + \left( Q_{s,mn,t}^{\text{flow,ac}} \right)^2 \right) / v_{s,m,t}, \quad \forall m, n \in N_{\text{ac}} \quad (32)$$

$$I_{s,mn,t}^{\text{dc}} = \left( P_{s,mn,t}^{\text{flow,dc}} \right)^2 / v_{s,m,t}, \forall m, n \in N_{\text{dc}} \quad (33)$$

where  $v_{s,n,t} \triangleq V_{s,n,t}^2$ ,  $I_{s,mn,t}^{\text{ac/dc}} = (I_{s,mn,t}^{\text{ac/dc}})^2$

$$V_{s,n,t}^{\text{VSC,ac}} = 0.612 M_{s,n,t} V_{s,n,t}^{\text{VSC,dc}} \quad (34)$$

$$P_{s,n,t}^{\text{VSC,ac}} + P_{s,n,t}^{\text{VSC,dc}} + P_{s,n,t}^{\text{VSC,loss}} = 0, \forall s \quad (35)$$

$$\left( P_{s,n,t}^{\text{VSC,ac}} \right)^2 + \left( Q_{s,n,t}^{\text{VSC,ac}} \right)^2 = \left( P_{s,n,t}^{\text{VSC,loss}} / \nu^{\text{VSC}} \right)^2 \quad (36)$$

$$P_{s,n,t}^{\text{VSC,dc}} = \eta_{\text{VSC}} P_{s,n,t}^{\text{VSC,ac}} \quad (37)$$

$$\left( P_{s,n,t}^{\text{VSC,ac}} \right)^2 + \left( Q_{s,n,t}^{\text{VSC,ac}} \right)^2 \leq (\bar{S}_n^{\text{VSC}})^2 \quad (38)$$

$$\left( P_{s,mn,t}^{\text{flow,ac/dc}} \right)^2 + \left( Q_{s,mn,t}^{\text{flow,ac}} \right)^2 \leq (\bar{S}_{mn}^{\text{flow}})^2, \forall m, n \in N \quad (39)$$

$$P_{s,t}^{\text{buy/sell}} = \left[ \begin{array}{l} \sum_{n \in N_{\text{ac}}} P_{s,n,t}^{L,\text{net,ac}} + \sum_{n \in N_{\text{dc}}} P_{s,n,t}^{L,\text{net,dc}} \\ + \sum_{m \in N_{\text{ac}}} \sum_{n \in N_{\text{ac}}} r_{mn}^{\text{ac}} I_{s,mn,t}^{\text{ac}} \\ + \sum_{m \in N_{\text{dc}}} \sum_{n \in N_{\text{dc}}} r_{mn}^{\text{dc}} I_{s,mn,t}^{\text{dc}} + \sum_{n \in N} P_{s,n,t}^{\text{VSC,loss}} \end{array} \right] \quad (40)$$

$$Q_{s,t}^{\text{buy}} = \sum_{n \in N_{\text{ac}}} Q_{s,n,t}^{L,\text{net,ac}} + \sum_{m \in N_{\text{ac}}} \sum_{n \in N_{\text{ac}}} x_{mn}^{\text{ac}} I_{s,mn,t}^{\text{ac}} \quad (41)$$

AC network active and reactive power balance equations are depicted in (23) and (24), respectively. Constraint (25) represents dc network active power balance. Ohm's law constraint of ac and dc lines is constraints (26) and (27), respectively. Net power demand at ac and dc nodes is given in (28)–(30). Constraint (31) depicts the bus voltage magnitude boundaries. Power flow in ac and dc lines is represented in constraints (32) and (33), respectively. Relation between ac and dc side voltages of VSC are related with each other by following constraint (34) [39]. Constraint (35) is the active power balance equation at VSC station. Power loss at VSC is given by (36). AC and dc side power of VSC are related with each other by constraint (37). VSC can act in both rectifier and inverter operation modes but regardless of any operating mode VSC should follow constraint (37) [39]. Capacity constraint of VSC station is denoted in (38). Line flow capacity is given in (39). Equations (40) and (41) represent the substation active and reactive power balance.

### E. Optimization Objective Function

The primary objective of the ADNMS is to minimize the overall expected energy cost as follows:

$$\text{Min}_{\Omega} C(\Omega) = \sum_{s \in S} \rho_s \left( \sum_{t \in T} \left( P_{s,t}^{\text{buy}} r_{s,t}^{\text{buy}} - P_{s,t}^{\text{sell}} \varphi r_{s,t}^{\text{buy}} \right) \Delta t \right), \quad 0 \leq \varphi < 1 \quad (42)$$

Subject to (1)–(41) and

$$P_{s,t}^{\text{buy}} \leq \lambda_t^{\text{buy}} P^{\text{max}} \text{ and } P_{s,t}^{\text{sell}} \leq (1 - \lambda_t^{\text{buy}}) P^{\text{max}} \quad (43)$$

Overall scenario probability,  $\rho_s = \rho_s^{\text{PV}} \times \rho_s^{L,F} \times \rho_s^{\text{buy}}$  and  $\Omega$  is set of decision variables.

The energy buy price uncertainty is modeled as Normal distribution as follows:

$$f(r_t^{\text{buy}}) = \frac{1}{\sigma_t^{\text{buy}} \sqrt{2\pi}} \exp \left( -\frac{1}{2} \left( \frac{r_t^{\text{buy}} - \mu_t^{\text{buy}}}{\sigma_t^{\text{buy}}} \right)^2 \right) \quad (44)$$

It is pertinent to mention here that minimization of expected energy cost is beneficial compared to the deterministic framework where forecasted solar generation, load, and energy price are considered to be error free and distribution of the outcomes due to individual scenario is neglected. However, an allowable amount of expected energy cost can have a distribution curve in which the probability of occurrence of higher cost values corresponding to some certain scenarios is more. To avoid such issues, idea of risk must be included in the optimization framework to measure the risk associated with the optimal expected energy cost.

VaR is quite famous risk measurement strategy but lack in subadditivity and convexity makes it unsuitable for adding in optimization problems [40]. In this regards, CVaR, proposed by Rockafellar and Uryasev [40], and outperforms VaR because of following features: 1) compared to VaR, CVaR quantifies a cost distribution having “fat tails”, 2) its linear formulation makes it compatible with MILP frameworks, and 3) it is a rational measurement of risk.

For  $C(\Omega)$  energy cost function, VaR at probability level  $\alpha \in [0, 1]$  is defined as the minimum expected energy cost  $\beta$ , such as the cost values above  $\beta$  have at most probability of  $(1-\alpha)$ . Therefore, mathematically VaR can be expressed as

$$\alpha - \text{VaR} \triangleq \min [\beta : P(C(\Omega) \leq \beta) \geq \alpha], 0 \leq \alpha \leq 1 \quad (45)$$

Now, as per [40], CVaR is defined as the conditional expected cost above  $\alpha$ -VaR and this is given by

$$\alpha - \text{CVaR} \triangleq \min \left[ \beta + \frac{1}{1-\alpha} \sum_{s \in S} [\rho_s \times \max(C(\Omega) - \beta, 0)] \right] \quad (46)$$

The above CVaR value can be converted to its linear counterparts by using auxiliary variables  $Z_s$ , such that

$$\alpha - \text{CVaR} = \beta + \frac{1}{1-\alpha} \sum_{s \in S} [\rho_s Z_s] \quad (47)$$

$$C(\Omega) - \beta \leq Z_s, \forall s \in S \text{ and } Z_s \geq 0, \forall s \in S \quad (48)$$

Therefore, both expected cost and CVaR minimization is considered in a single objective function as follows:

$$\text{Min}_{\Omega, \alpha, (Z_s, \forall s)} (1-\gamma) C(\Omega) + \gamma(\alpha - \text{CVaR}), 0 \leq \gamma \leq 1 \quad (49)$$

subject to (1)–(41), (43), (44), and (48).

### III. SOLUTION PROCESS

#### A. Two-Point Estimation (2PE) Method

Conventionally, the scenario generation from pdfs in case of stochastic optimization is carried out using MCS because of its simple implementation. MCS quantifies the uncertainty by extracting random scenarios from the pdfs. With the help of MCS, few hundreds or thousands of scenarios are generated to obtain more accurate decisions. However, increment in scenarios enhances the total number of decision variables and constraints in the optimization portfolio, and that lengthens solution time and increase computation burden. To get rid of that, MCS is merged with scenario reduction techniques to reduce the

computation burden but determination of optimal number of scenarios from scenario reduction technique is difficult task. For simple but effective solution process, in this article, 2PE method proposed by [41] is implemented to approximate the entire pdf of the uncertain parameters at each time step at two concentrated locations by using (50)–(53). This will reduce the computation process and time significantly as unlike MCS-based method, in this case, only two concentrated but effective scenarios are evaluated in the risk constrained optimization framework.

Suppose, for a set of random parameters  $P$ ,  $f(P)$  is the pdf having mean at  $\mu_P$  and standard deviation at  $\sigma_P$ . Then, two condensed locations are determined by (50) [41]:

$$p_s = \mu_P + \xi_s \sigma_P, \forall s = 1, 2 \quad (50)$$

where

$$\xi_s = (\lambda_{P,3}/2) + (-1)^{3-s} \sqrt{1 + (\lambda_{P,3}/2)^2} \quad (51)$$

Probability of each scenario “s” is given by

$$\rho_s = ((-1)^s \xi_{3-s}) / \left( 2\sqrt{1 + (\lambda_{P,3}/2)^2} \right) \quad (52)$$

$\lambda_{P,3}$  is skewness coefficient of the pdf and it is given by

$$\lambda_{P,3} = M_3(P) / \sigma_P^3 \quad (53)$$

Here,  $M_3(P)$  is third-order central moment of pdf.

Therefore, implementing the idea of 2PE, the risk constrained optimization framework is revised as

$$\text{Min}_{\Omega, \alpha, (Z_s, \forall s)} (1-\gamma) C(\Omega) + \gamma(\alpha - \text{CVaR}), \forall s = 1, 2 \quad (54)$$

subject to (1)–(41), (43), (44), (48), and (50)–(53).

#### B. Linearization

The above derived problem is strictly nonconvex due to presence of absolute functions, bilinear terms, and quadratic expressions in some constraints, and hence it is NP-hard to solve. To simplify the solution process, here some linearization techniques are applied to reformulate the nonconvexities as described below.

1) *Approximation of Absolute Functions (|·|)*: Absolute functions are present in the constraints (20) and (22). The linearization process is described below. Any absolute function  $|x - y|$  can be linearized by defining auxiliary variable

$$H = |x - y| \quad (55)$$

such that

$$H \geq 0, H \geq x - y, \text{ and } H \geq y - x \quad (56)$$

Hence,

$$\begin{aligned} \sum_{t \in T} H_{n,t}^{\text{VR}} &\leq N T_n^{\text{VR}}, H_{n,t}^{\text{VR}} \geq T_{n,t}^{\text{VR}} - T_{n,t-1}^{\text{VR}} \text{ and } H_{n,t}^{\text{VR}} \\ &\leq T_{n,t}^{\text{VR}} - T_{n,t-1}^{\text{VR}} \end{aligned} \quad (57)$$

$$\begin{aligned} \sum_{t \in T} H_{n,t}^{\text{CB}} &\leq N S_n^{\text{CB}}, H_{n,t}^{\text{CB}} \geq S W_{n,t}^{\text{CB}} \\ &- S W_{n,t-1}^{\text{CB}} \text{ and } H_{n,t}^{\text{CB}} \leq S W_{n,t}^{\text{CB}} - S W_{n,t-1}^{\text{CB}} \end{aligned} \quad (58)$$



2) *Approximation of Bilinear Terms*: Bilinear terms present in (5), (6), and (34) due to multiplication of two continuous decision variables. These bilinear terms take form as “ $xy$ ,”  $x \in [x^L, x^U]$ , and  $y \in [y^L, y^U]$ . This can be linearized by creating McCormick envelopes for an auxiliary variable “ $H$ ” as follows [42]:

$$H \geq \max(xy^U + x^U y - x^U y^U, xy^L + x^L y - x^L y^L) \quad (59)$$

$$H \leq \min(xy^U + x^L y - x^L y^U, xy^L + x^U y - x^U y^L) \quad (60)$$

However, these envelopes suffer from tightness issues if the range of the variables is very large [43]. Therefore, here McCormick envelopes are applied on the per unit values of the variables to revise (5), (6), and (34) as follows:

$$P_{s,n,t}^{L,cvr} / S_{base} = Z_P H_{s,n,t}^{L1} + I_P H_{s,n,t}^{L2} + P_P (P_{s,n,t}^L / S_{base}) \quad (61)$$

$$Q_{s,n,t}^{L,cvr} / S_{base} = \left( \sqrt{(1/pf_n^2) - 1} \right) (Z_Q H_{s,n,t}^{L1} + I_Q H_{s,n,t}^{L2} + P_Q (P_{s,n,t}^L / S_{base})) \quad (62)$$

$$V_{s,n,t}^{VSC,ac} = 0.612 H_{s,n,t}^{VSC} V_{nom}^{dc} \quad (63)$$

subject to the revised constraints of (59) and (60) considering

$$H_{s,n,t}^{L1} = (P_{s,n,t}^L / S_{base}) w_{s,n,t}, H_{s,n,t}^{L2} = (P_{s,n,t}^L / S_{base}) u_{s,n,t}$$

and

$$H_{s,n,t}^{VSC} = M_{s,n,t} \left( V_{s,n,t}^{VSC,dc} / V_{nom}^{dc} \right).$$

Another type of bilinear terms in expression (21) is due to multiplication of one binary and one continuous variables. This nonconvexity can be relaxed by rewriting the expression as (64) with an auxiliary variable  $H_{n,t}^{CB}$ :

$$Q_{s,n,t}^{CB} = H_{n,t}^{CB} \bar{Q}_n^{CB} \quad (64)$$

such that

$$(V_{n,min})^2 SW_{n,t}^{CB} \leq H_{n,t}^{CB} \leq (V_{n,max})^2 SW_{n,t}^{CB} \quad (65)$$

$$v_{s,n,t} - (V_{n,max})^2 (1 - SW_{n,t}^{CB}) \leq H_{n,t}^{CB} \leq v_{s,n,t} - (V_{n,min})^2 (1 - SW_{n,t}^{CB}) \quad (66)$$

3) *Approximation of Quadratic Expressions*: It is noticed from [25] and [30] that SOCP relaxation of quadratic equalities can solve the nonconvex problem in an acceptable accuracy. However, the solution time is long. In this article, quadratic equality constraints (32), (33), (36) and inequality constraints (17), (38), (39) are approximated as their linear counterparts (67)–(72), respectively, by replacing each quadratic term by their corresponding first-order Taylor series, evaluated at solution

point at iteration  $k$  [denoted by a hat (^)]:

$$2P_{s,mn,t}^{flow,ac} \left( \hat{P}_{s,mn,t}^{flow,ac} \right)^g + 2Q_{s,mn,t}^{flow,ac} \left( \hat{Q}_{s,mn,t}^{flow,ac} \right)^g - \left[ \left( \hat{P}_{s,mn,t}^{flow,ac} \right)^g \right]^2 - \left[ \left( \hat{Q}_{s,mn,t}^{flow,ac} \right)^g \right]^2 = l_{s,mn,t}^{ac} (\hat{v}_{s,m,t})^g + v_{s,m,t} \left( \hat{l}_{s,mn,t}^{ac} \right)^g - \left( \hat{l}_{s,mn,t}^{ac} \right)^g (\hat{v}_{s,m,t})^g \quad (67)$$

$$2P_{s,mn,t}^{flow,dc} \left( \hat{P}_{s,mn,t}^{flow,dc} \right)^g - \left[ \left( \hat{P}_{s,mn,t}^{flow,dc} \right)^g \right]^2 = l_{s,mn,t}^{dc} (\hat{v}_{s,m,t})^g + v_{s,m,t} \left( \hat{l}_{s,mn,t}^{dc} \right)^g - \left( \hat{l}_{s,mn,t}^{dc} \right)^g (\hat{v}_{s,m,t})^g \quad (68)$$

$$2P_{s,n,t}^{VSC,ac} \left( \hat{P}_{s,n,t}^{VSC,ac} \right)^g + 2Q_{s,n,t}^{VSC,ac} \left( \hat{Q}_{s,n,t}^{VSC,ac} \right)^g - \left[ \left( \hat{P}_{s,n,t}^{VSC,ac} \right)^g \right]^2 - \left[ \left( \hat{Q}_{s,n,t}^{VSC,ac} \right)^g \right]^2 = (1/\nu^{VSC})^2 \times \left[ 2P_{s,n,t}^{VSC,loss} \left( \hat{P}_{s,n,t}^{VSC,loss} \right)^g - \left[ \left( \hat{P}_{s,n,t}^{VSC,loss} \right)^g \right]^2 \right] \quad (69)$$

$$2P_{s,n,t}^{bat,ch/dch} \left( \hat{P}_{s,n,t}^{bat,ch/dch} \right)^g + 2Q_{s,n,t}^{bat} \left( \hat{Q}_{s,n,t}^{bat} \right)^g - \left[ \left( \hat{P}_{s,n,t}^{bat,ch/dch} \right)^g \right]^2 - \left[ \left( \hat{Q}_{s,n,t}^{bat} \right)^g \right]^2 \leq (\bar{S}_n^{bat})^2 \quad (70)$$

$$2P_{s,n,t}^{VSC,ac} \left( \hat{P}_{s,n,t}^{VSC,ac} \right)^g + 2Q_{s,n,t}^{VSC,ac} \left( \hat{Q}_{s,n,t}^{VSC,ac} \right)^g - \left[ \left( \hat{P}_{s,n,t}^{VSC,ac} \right)^g \right]^2 - \left[ \left( \hat{Q}_{s,n,t}^{VSC,ac} \right)^g \right]^2 \leq (\bar{S}_n^{VSC})^2 \quad (71)$$

$$2P_{s,mn,t}^{flow,ac/dsc} \left( \hat{P}_{s,mn,t}^{flow,ac/dc} \right)^g + 2Q_{s,mn,t}^{flow,ac} \left( \hat{Q}_{s,mn,t}^{flow,ac} \right)^g - \left[ \left( \hat{P}_{s,mn,t}^{flow,ac/dc} \right)^g \right]^2 - \left[ \left( \hat{Q}_{s,mn,t}^{flow,ac} \right)^g \right]^2 \leq (\bar{S}_{mn}^{flow})^2 \quad (72)$$

### C. Overall ADNMS Framework

The overall proposed ADNMS optimization framework of ac/dc HDN is given by ADNMS:

$$\begin{cases} \text{Min}_{\Omega, \alpha, (Z_s, V_s), H} (1 - \gamma) C(\Omega) + \gamma (\alpha - CVaR), \forall s = 1, 2 \\ \text{subject to, (1)–(4), (7)–(16), (18), (19), (23)–(31), (35), (37), (40), (41), (43), (44), (48), (50)–(53), (57)–(72)} \end{cases}$$

$H$  is set of auxiliary variables. As can be seen that the objective function and all revised constraints are linear counterparts of their corresponding nonlinear expressions. Therefore, the ADNMS problem takes form of an easily solvable MILP.

### D. Successive MILP Solution Process

It is noticed that due to the first-order Taylor series expressions (67)–(72), the derived linear optimization framework should

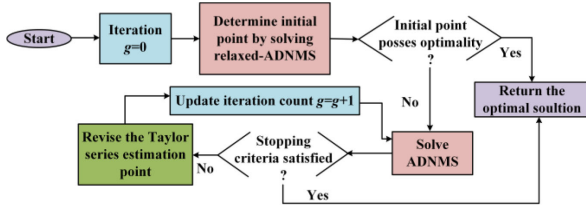


Fig. 2. Successive MILP (s-MILP) approach for solving ADNMS of ac/dc HDN.

be solved multiple times to get optimal solutions. The flow chart of the proposed sequential MILP approach for solving ADNMS of ac/dc HDN is portrayed in Fig. 2. For starting the iteration, initial evaluation point determination for (67)–(72) is a critical job, as erroneous choice of starting point can lead to local optimum solution. To avoid this, in this article, the initial point is determined by adopting the continuous relaxation process where relaxed-ADNMS, defined below, is solved considering all the decision variables as continuous type. This approach will reduce the chance of sticking at local optimum as solution point of relaxed-ADNMS will be nearer to the optimal point of the original problem.

Relaxed-ADNMS:

$$\begin{cases} \text{Min}_{\Omega, \alpha, (Z_s, \forall s), H} (1 - \gamma) C(\Omega) + \gamma(\alpha - \text{CVaR}), \forall s = 1, 2 \\ \text{subject to, (1)–(4), (7)–(19), (23)–(41), (43),} \\ (44), (48), (50)–(53), (57)–(66) \end{cases}$$

If the initial point possesses optimality, then the solution is returned else the iteration process starts and continues till the difference between optimal value of objective function for consecutive two iterations are within the tolerance limit ( $1e-4$ ). After termination of the iterative process, the returned outcomes can be of three types viz. 1) global optimal solution, 2) solution is feasible but not global, and 3) infeasible solution. Outcome 3 stipulates that either the initial point is not proper or the problem is unbounded or the problem does not have any feasible solution. Solution type 1 and 2 are meaningful, however to avoid type 2, in this article, initial point is derived by solving relaxed-ADNMS.

#### IV. CASE STUDY

##### A. IEEE 33 Bus AC/DC Hybrid Distribution Network Data

In this article, IEEE 33 bus ac/dc HDN described in [33] is considered for demonstrating the proposed ADNMS topology. The base MVA of the network is 10 MVA, base voltages for ac and dc networks are 12.66 and 20.67 kV, respectively. The substation bus (bus 1) voltage is considered to be fixed at 1.0 pu. The network has been modified by placing two solar panels, two batteries, and two CBs at the bus locations shown in Fig. 3. One VR is placed between buses 4 and 5 which has 32 tap positions and can perform at most 60 tap changing operations in a day [44]. The bus voltage magnitudes are allowed to vary within 0.95 to 1.05 pu according to their respective base values. Solar panels are of 1 MW capacity each and every batteries are of 1 MWh–0.5 MW rating, 95% efficient, and can discharge up to 30% of its capacity. Initially, batteries are at their 50% energy level. CBs are

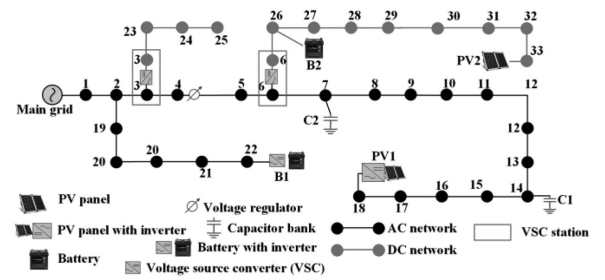


Fig. 3. Modified IEEE 33 bus ac/dc HDN.

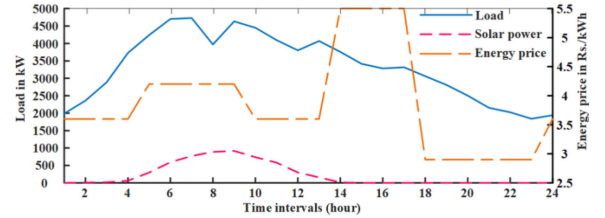


Fig. 4. Input load, solar generation, and energy price data for simulation.

of 100 kVAR capacity and can be switched ON/OFF at most six times in one day [44]. Solar generation from a practical PV panel is uplified to the scale of 1 MW for simulation. Solar generation from each panel, 24-h load curve of the entire network (from 6 am of present day to 6 am of next day), and the dynamic energy price data from literature [33] are portrayed in Fig. 4. Power factor of the ac buses are assumed to be remained same at each time interval as the base case power factor. Per hour shiftable load demand at each bus is considered randomly between 50% and 70% of the total forecasted load demand. Efficiency of VSCs is 95% and they operate at 0.95 power factor. Both solar and battery inverters are of 1.5 MVA ratings. The value of  $\alpha$  is set to 0.9. Mean value of the pdfs is set to the forecasted nominal value and SD is equal to three times square root of the mean value [11].

##### B. Benefits of AC/DC Hybrid Distribution Network

In this section, the benefits of the ac/dc hybrid distribution is evaluated by comparing the ac/dc network shown in Fig. 3 with the standard IEEE 33 bus ac distribution network with the same load profile (as shown in Fig. 4) and DERs. The simulation is carried out without considering CVR and LS operations (i.e., constant power load model is considered) and the uncertainties. Therefore, the objective function is set to reduce the deterministic value of the total monetary energy cost for the entire day. It is worthy to say that in the ac network, dc energy sources PV2 and B2 in Fig. 3 are connected through dc–ac converters of 95% efficiency (the efficiency is accounted same as VSC to show the comparison results properly). The simulation outcomes related to hourly monetary energy cost and total active power loss (sum of network loss and power conversion loss) for the two networks are shown in Table I. It is noted from Table I that at the instants of high renewable generation from PV2 (hours 10 to 5 pm) or discharging hours of B2 (intervals 14 and 17), ac/dc HDN

TABLE I  
COMPARATIVE ANALYSIS BETWEEN AC AND AC/DC NETWORKS

Hours	AC Network		AC/DC HDN	
	Power loss (kW)	Monetary energy cost (Rs.)	Power loss (kW)	Monetary energy cost (Rs.)
1 (6:00 am)	72.145	7845.03	75.393	7857.03
2 (7:00 am)	80.803	9644.37	84.128	9657.42
3 (8:00 am)	103.806	12905.32	99.666	12890.41
4 (9:00 am)	103.39	11543.46	71.155	11427.42
5 (10:00 am)	119.840	14688.48	93.689	14578.66
6 (11:00 am)	134.939	14900.04	97.890	14744.44
7 (12:00 am)	143.906	14206.68	95.184	14002.05
8 (1:00 pm)	154.796	9408.94	96.487	9164.04
9 (2:00 pm)	166.843	10533.25	101.685	10259.59
10 (3:00 pm)	150.271	12946.34	93.762	12742.9
11 (4:00 pm)	128.190	12089.9	81.338	11921.23
12 (5:00 pm)	118.579	14263.37	80.750	14127.19
13 (6:00 pm)	75.03	13790.15	57.905	13728.5
14 (7:00 pm)	112.92	15657.73	78.465	15468.23
15 (8:00 pm)	91.709	19447.76	92.842	19453.99
16 (9:00 pm)	87.993	18462.36	84.135	18441.14
17 (10:00 pm)	91.796	16465.62	73.477	16364.87
18 (11:00 pm)	83.54	9116.77	87.09	9127.07
19 (12:00 am)	105.436	9522.18	106.362	9524.87
20 (1:00 am)	91.029	8082.76	92.547	8087.16
21 (2:00 am)	78.321	6718.34	81.282	6726.93
22 (3:00 am)	83.632	6679.92	85.897	6686.49
23 (4:00 am)	103.302	7255.88	105.231	7261.48
24 (5:00 am)	65.25	3626.50	54.38	3587.36
<b>Total</b>	<b>2547.17</b>	<b>279801.5</b>	<b>2070.74</b>	<b>277830.5</b>

achieves notable reduction in both loss and monetary energy cost. Maximum hourly reduction for active power loss of 65.16 kW and cost of 273.66 Rs. are noticed at hour 2 pm (interval 9). At some hours, when renewable generation is very low and the battery B2 is in charging mode, power losses in the ac network is lesser than ac/dc HDN (hours 11:00 pm to 4:00 am). However, for the entire time period of 24 h, the total loss and energy cost for ac networks are 2547.17 kW and 279801.5 Rs., respectively, and for ac/dc HDN those values are 2070.74 kW and 277830.5 Rs., respectively. Hence, it is pertinent to conclude that for the entire day of operation, ac/dc HDN is much beneficial than only ac network and that results 18.70% and 0.704% reduction in total loss and energy cost, respectively.

C. Simulation Results

The simulation is carried out using MILP solver present at MATLAB 2019b in an i7, 64 bit, 16 GB RAM personal computer. Initially, value of  $\gamma$  is set to 0.5 and the loads are considered to be of residential type whose ZIP coefficients are taken from [45]. Relaxed-ADNMS is solved using non-linear programming commercial solver present in MATLAB.

For demonstrating the effectiveness of merging LS and CVR, four cases viz. 1) No LS, No CVR, 2) No LS, Yes CVR, 3) Yes LS, No CVR, and 4) Yes LS, Yes CVR are simulated and the outcomes related to total load demand are portrayed in Fig. 5. Table II depicts the solutions at minimum and maximum loading conditions for each case. To simulate case 1, the voltage magnitude boundary limits are relaxed from 0.9 to 1.1 pu to get feasible solution with the considered load demand profile. It is

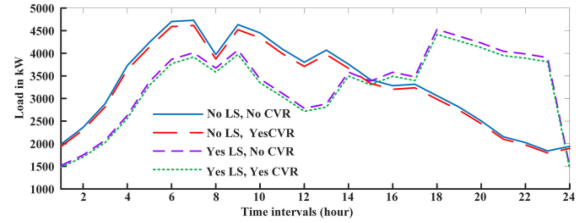


Fig. 5. Effect of load shifting and CVR on the load demand.

TABLE II  
ADNMS OUTCOMES FOR DIFFERENT CASES

Parameter	Case	Maximum load	Minimum load
Load (kW)	1	4730.4	1839.89
	2	4616.5	1794.8
	3	4528.95	1492.41
	4	4417.6	1455.4
VR tap position	4	8	5
C1 status	4	ON	ON
C2 status	4	ON	OFF
Maximum voltage (pu)	1	0.962	0.991
	2	0.975	0.989
	3	0.977	0.994
	4	0.972	0.990
Minimum voltage (pu)	1	0.934	0.959
	2	0.951	0.958
	3	0.956	0.978
	4	0.950	0.954

TABLE III  
TOTAL OPERATIONS OF VVC DEVICES OVER THE DAY

Parameter	Case 1	Case 2	Case 3	Case 4
VR tap operations	46	54	58	49
C1 switching operations	5	5	5	5
C2 switching operations	6	5	5	4

seen that in absence of both LS and CVR (case 1), the peak load is maximum and that causes the minimum bus voltage go below the tolerance limit (i.e., 0.95 pu). By leveraging the benefit of voltage dependent load models, in case 2 peak load reduction of 2.4% is obtained by setting the minimum voltage magnitude at the lower boundary. LS process alone (case 3) can successfully shift the demand from peak load hours to off-peak hours (Fig. 5) and causes 4.25% peak reduction (Table II). Deployment of CVR with LS (case 4) further reduces the demand by reducing the consumption of voltage dependent loads and that results a total peak demand reduction of 6.61% from that of case 1. However, same as case 2 CVR deployment brings the minimum bus voltage magnitudes close to its minimum boundary limit for getting maximum benefit at case 4. From Table II, it is noted that the VR tap positions and CB switching status change with the loading conditions. Table III shows that for cases 2 to 4, the bus voltages are kept within safety limits by performing more number of tap changing operations in VR compared to case 1. However, as the total number of tap and switching operations are within the safety limit, then it is worthy to mention that the most energy efficient operation is obtained by merging both LS and CVR in the ADNMS process.

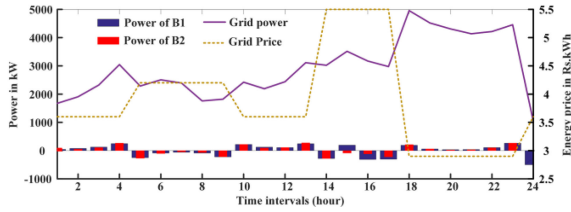


Fig. 6. Simulation output of ADNMS in terms of battery power and grid power consumption.

TABLE IV  
PEAK LOAD FOR DIFFERENT LOAD MIX

Load mix	Case 1	Case 2	Case 3	Case 4
100% R	4730.4	4616.5	4528.95	4417.6
75% R, 25% SC	4730.4	4678.4	4586.3	4473.6
50% R, 50% SC	4730.4	4702.3	4619.8	4526.7

The simulation results regarding battery charging/discharging power and grid power consumption are shown in Fig. 6 along with the energy price. It is noted that the total hourly load demand is satisfied coordinately by solar panels, batteries, and the main grid. During more solar generation hours, i.e., intervals 5 to 9 (10 am to 2 pm) grid consumption reduced and a major portion of the load demand is satisfied by the battery discharging power and the generated solar energy. During solar generation hours, battery discharges (10 am to 2 pm) due to high energy price (mid-peak energy price hours). During 3 pm to 6 pm intervals 10 to 13), energy prices are comparatively low, hence ADNMS charges the batteries which are further discharged during the peak energy price hours (i.e., intervals 14 to 17 or 7 pm to 10 pm). Finally, to satisfy the constraint (16), i.e., to bring the battery status at the initial level, during off-peak energy price hours, the batteries are again charged. Battery charging at off-peak price hours and discharging at peak price hours demonstrate the effectiveness of the proposed ADNMS strategy and hence it is concluded that power dispatch from various energy resources are optimized to get lowest energy cost.

McCormick envelopes are used for replacing the bilinear nonconvexities. However, as mentioned in Section III-B, this envelope suffers from tightness issues if range of the variables is large. Hence, in this article, envelopes are designed for per unit values of the variables, which are approximately tight and cause maximum mismatch of 0.04% for the entire simulation period. Whereas, if the envelopes are created on the actual values of the variables, maximum mismatch of 6.57% is obtained. Therefore, it can be judged that the envelope approximations are quite trustworthy and applicable if applied on per unit values, which is done in this article.

Further investigation is carried out for different load mix scenarios at each bus with different percentage of residential (R) and small commercial (SC) loads and the result in terms of peak demand are depicted in Table IV. The ZIP coefficients for SC loads are taken from [45]. It is noticed that as SC loads are less sensitive to the phase voltage magnitude compared to R loads, the peak load reduction is lower if the share of SC load is more.

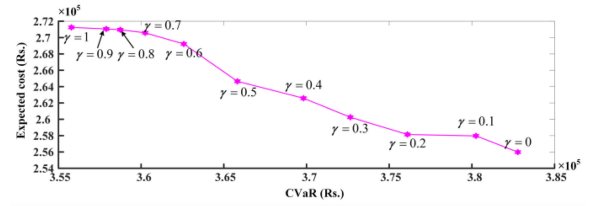


Fig. 7. Impact of risk aversion parameter on cost.

TABLE V  
COMPARISON BETWEEN 2PE AND MCS METHODS

Scenario generation method	Number of scenarios	Expected cost (Rs.) ( $\times 10^5$ )	CVaR (Rs.) ( $\times 10^5$ )	Computation time (min)
MCS	1000	2.6388	3.6536	625.85
MCS+BSR	500	2.6402	3.6545	341.51
	200	2.6438	3.6463	257.89
	100	2.6455	2.6578	128.10
	50	2.6475	2.6585	95.47
	10	2.6487	2.6593	79.14
2PE	2	2.6465	3.6582	52.51

To study the impact of the risk-constrained study on the ADNMS design, risk aversion parameter “ $\gamma$ ” is varied between 0 and 1, and the values of expected cost and CVaR are noted. The plot for CVaR vs. expected cost is portrayed in Fig. 7. It is noticed that as the value of  $\gamma$  increases, the CVaR decreases and the expected cost of the ac/dc HDN increases.

#### D. Effectiveness of 2PE Process

Conventionally, stochastic optimization frameworks are designed by generating scenarios from MCS process followed by scenario reduction techniques. However, computation complexity of stochastic optimization becomes worse with increasing number of scenarios. To prove the effectiveness of the 2PE process, further investigation is carried out with MCS followed by backward scenario reduction (BSR) technique considering loads as residential type and  $\gamma = 0.5$  and solution is carried out using s-MILP approach. Initially, 1000 samples are generated from MCS to obtain the original optimal point and then with the help of BSR process 1000 scenarios are reduced to 10, 50, 100, 200, and 500 scenarios. The value of expected cost and CVaR for the above cases is listed in Table V with their computation time and compared with the proposed 2PE based ADNMS. It is noted that the actual solution with 1000 scenarios possess highest computation time due to occurrence of large number of constraints in the optimization process. Both accuracy and computation time gradually reduce if scenario reduction technique is adopted after MCS for decreasing total number of scenarios. However, if the scenario number is reduced below 50 using BSR, then the solution point deviate significantly from the original optimal point. On contrary, 2PE-based solution process require comparatively very less time and the optimal solution also does not deviate much from the actual solution. Therefore, it is pertinent to mention here that the 2PE process converges nearly to the same optimum point and also possess fast convergence.

TABLE VI  
COMPARISON BETWEEN DIFFERENT SOLUTION APPROACHES

Method	Number of segments	Objective function value (Rs.) ( $\times 10^5$ )	Error	Computation time (min)
MICP (OA)	-	3.1498	-	148.69
Piecewise linearization	2	3.1952	1.44%	29.78
	6	3.1585	0.276%	33.54
	10	3.1536	0.121%	46.98
	12	3.1519	0.067%	67.46
	14	3.1517	0.060%	76.13
s-MILP	-	3.1524	0.082%	52.51

### E. Computation Efficacy Evaluation of s-MILP

To establish the superiority of the s-MILP approach in terms of accuracy and computational time, in this section, the outcomes are compared with two major solution approaches found from the literatures viz. SOCP relaxed MICP and piecewise linearization based MILP and the outcomes are depicted in Table VI.

Generally quadratic equalities (32), (33), and (36) are converted to SOCP relaxed inequalities to convert the MINCP framework to a simple MICP because SOCP relaxations can determine the optimal power flow solutions within acceptable accuracy [27]. Here, the MICP is solved using outer approximation (OA) process due to its superiority among all decomposition methods present for solving MICP [46]. The outcome of this MICP optimization framework will serve as the reference to validate the convergence of different solution techniques in terms of both accuracy and solution time. It is noted that the MICP problem takes almost 2.5 h time to converge because OA method solves a convex optimization problem at each iteration as a subproblem of a relaxed master MILP problem.

Another solution process for MINCP is to linearize the quadratic terms with the help of piecewise linearization process by representing every quadratic term in equality constraints (32), (33), (36) and inequality constraints (17), (38), (39) with a set of segmented linear curves. In this article, the number of segments is varied from 2 to 14 and the outcomes are shown in Table VI. Again, the bilinear terms present in the expressions (32) and (33) is linearized with the help of McCormick envelopes applied on the per unit values of the variables. It is noted that although accuracy of solution process increases with the increasing number of segments but that also lengthens the solution time due to addition of extra decision variables and constraints in the optimization framework. Again, for number of segments above 12, the accuracy level becomes stable.

Compared to the abovementioned two MINCP solution techniques, proposed s-MILP approach performs better. The error is only 0.082% whereas the computation time is around 52 min. Though the computation time of s-MILP is more compared to piecewise linearization based MILP with 2, 6, and 10 segments due to multiple time solution of linear ADNMS framework, but error reduction is also significant from the above three cases. Compared to piecewise technique with 12 and 14 segments, though the obtained error for s-MILP is more but the computation time is sufficiently low.

TABLE VII  
COMPARISON WITH THE ACTUAL BENCHMARK METHOD

Method	Expected cost (Rs.) ( $\times 10^5$ )	CVaR (Rs.) ( $\times 10^5$ )	Objective function value (Rs.) ( $\times 10^5$ )	Error	Computation time (min)
MCS+MICP	2.6238	3.6377	3.1308	-	957.32
2PE+s-MILP	2.6465	3.6582	3.1524	0.69%	52.51

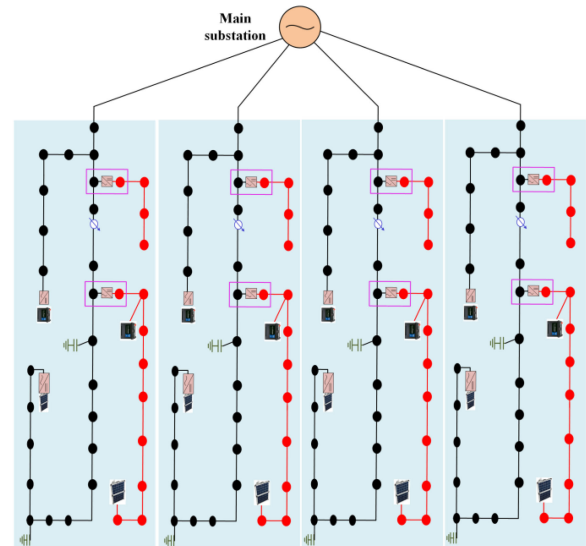


Fig. 8. 132 bus ac/dc hybrid distribution network for scalability checking.

### F. Overall Accuracy Assessment of the Proposed ADNMS

To evaluate the overall accuracy of the proposed technique, a benchmark solution is determined by solving the proposed ADNMS in SOCP relaxed MICP framework, where 1000 scenarios are generated from MCS. The outcomes of the benchmark method are considered to be the exact optimal solution of the nonconvex ADNMS. The comparison results are shown in Table VII with only residential loads and  $\gamma = 0.5$ . It is noted that the overall error incurs in the proposed technique is approximately 0.69%; however, the actual benchmark method takes almost 16 h to provide the optimal decision, which is very large. Therefore, it is worthy to conclude that the proposed strategy can provide good optimal solution within comparatively less time, which makes it adaptable for real life implementation.

### G. Scalability Checking of ADNMS

To perform scalability checking of the proposed ADNMS and s-MILP approach, further simulation is carried out on 132 bus ac/dc HDN shown in Fig. 8. The 132 bus network is formed by connecting four 33 bus ac/dc HDN to a common main distribution substation, where the centralized ADNMS is performed. This kind of architecture is considered in [16] for scalability checking of power flow algorithm for ac/dc HDN. The simulation results are shown in Table VIII for both MICP framework, where 1000 scenarios are generated from MCS

TABLE VIII  
SIMULATION OUTCOMES OF 132 BUS AC/DC HDN

Parameters	Solution method	
	MCS+MICP	2PE+s-MILP
Expected cost (Rs.) ( $\times 10^5$ )	11.1486	11.3386
CVaR (Rs.) ( $\times 10^5$ )	15.6782	15.8751
Objective function value (Rs.) ( $\times 10^5$ )	13.4134	13.6068
Error	-	1.43%
Computation time (min)	2389.8 (39.83 hours)	293.4 (4.89 hours)

and the proposed 2PE-based ADNMS, solved using s-MILP. It is noted that the proposed strategy can successfully converge near to the optimal point and the incurred error is only 1.43%. However, the computation time for MICP-based algorithm is more than 24 h (around 40 h) and that makes it unsuitable for day-ahead analysis. In contrast with that, the proposed technique generates optimal decisions for 132 bus system is around 5 h under previously mentioned computation facilities. Therefore, it is concluded that for day ahead analysis the proposed centralized scheme can efficiently converge for large ac/dc distribution grids and there is no need of network segmentation, i.e., division of the large network into different ac and dc subnetworks.

## V. CONCLUSION

This article elucidates a centralized risk-constrained advanced energy management topology for ac/dc HDNs by merging LS and CVR techniques. The developed optimization framework aims to minimize both true and CVaR values of the expected energy cost to eliminate the risk associated with solar power generation, load demand, and upper grid energy price uncertainties. To overcome the solution complexities, the nonconvex expressions are represented by their linear counterparts, formulated using auxiliary variable interpolation, McCormick envelopes and first-order Taylor series expansions. A successive MILP solution approach is proposed to solve the designed ADNMS strategy, where the initial evaluation point is determined by solving a continuous relaxation problem. After demonstrating on modified IEEE 33 bus ac/dc HDN, following conclusions are made:

- 1) The proposed ADNMS topology can provide most energy efficient operation while satisfying all security constraints for LS and CVR deployment.
- 2) Implementation of 2PE method in the proposed stochastic optimization portfolio causes significant reduction in the computation time compared to conventional MCS based portfolios without much compromising with the accuracy.
- 3) Proposed s-MILP performs well to solve MINCP-based ADNMS compared to existing SOCP relaxation and piecewise linearization based solution techniques as far as both error in optimal solution and computation time reductions are concerned.
- 4) The proposed technique can be applied to real life as it can generate nearly optimal solution within very less time. Scalability test on 132 bus ac/dc HDN proves the efficacy

and fast convergence of the proposed algorithm for large distribution networks.

The proposed centralized ADNMS strategy needs proper communication between the local resources and the central controller for information exchange which is the main impediment for successful deployment of the proposed topology. Again, the cyber networks are exposed under limited bandwidth and noises in the communication links [47], [48], and that will degrade the performance of the optimization process. As a future scope of research, the authors would like to extend their study for designing a robust energy management topology considering communication delays and uncertain communication links.

## REFERENCES

- [1] G. F. Reed, B. M. Grainger, A. R. Sparacino, and Z. H. Mao, "Ship to grid: Medium-voltage dc concepts in theory and practice," *IEEE Power Energy Mag.*, vol. 10, no. 6, pp. 70–79, Nov./Dec. 2012.
- [2] "Data and statistics," International Energy Agency, [Online]. Available: [https://www.iea.org/data-and-statistics?country=WORLD&fuel=Energy\\*\\*\\*\\*\\*%20consumption&indicator=CO2Industry](https://www.iea.org/data-and-statistics?country=WORLD&fuel=Energy*****%20consumption&indicator=CO2Industry)
- [3] "Paris agreement," Accessed: Dec. 2015. [Online]. Available: [http://ec.europa.eu/clima/policies/international/negotiations/paris/index\\_en.htm](http://ec.europa.eu/clima/policies/international/negotiations/paris/index_en.htm)
- [4] M. M. Hassan and E. K. Stanek, "Analysis techniques in AC/DC power systems," *IEEE Trans. Ind. Appl.*, vol. 17, no. 5, pp. 473–480, Sep./Oct. 1981.
- [5] "Insights into advanced distribution management systems," U.S. Dept. Energy, Washington, DC, USA, 2015, Accessed: 12 May 2018. [Online]. Available: [https://www.smartgrid.gov/files/ADMS-Guide\\_2-11.2015.pdf](https://www.smartgrid.gov/files/ADMS-Guide_2-11.2015.pdf)
- [6] S. R. Ghatak, S. Sannigrahi, and P. Acharjee, "Multiobjective framework for optimal integration of solar energy source in three-phase unbalanced distribution network," *IEEE Trans. Ind. Appl.*, vol. 56, no. 3, pp. 3068–3078, May/Jun. 2020.
- [7] A. Safdarian, M. Fotuhi-Firuzabad, and M. Lehtonen, "Benefits of demand response on operation of distribution networks: A case study," *IEEE Syst. J.*, vol. 10, no. 1, pp. 189–197, Mar. 2016.
- [8] A. Anilkumar, G. Devriese, and A. K. Srivastava, "Voltage and reactive power control to maximize the energy savings in power distribution system with wind energy," *IEEE Trans. Ind. Appl.*, vol. 54, no. 1, pp. 656–664, Jan./Feb. 2018.
- [9] H. Sheng, J. Xiao, Y. Cheng, Q. Ni, and S. Wang, "Short-term solar power forecasting based on weighted Gaussian process regression," *IEEE Trans. Ind. Electron.*, vol. 65, no. 1, pp. 300–308, Jan. 2018.
- [10] J. Wang, H. Zhong, X. Lai, Q. Xia, Y. Wang, and C. Kang, "Exploring key weather factors from analytical modeling toward improved solar power forecasting," *IEEE Trans. Smart Grid*, vol. 10, no. 2, pp. 1417–1427, Mar. 2019.
- [11] S. Paul and N. P. Padhy, "Resilient scheduling portfolio of residential devices and plug-in electric vehicle by minimizing conditional value at risk," *IEEE Trans. Ind. Inform.*, vol. 15, no. 3, pp. 1566–1578, Mar. 2019.
- [12] C. Zhao, S. Dong, F. Li, and Y. Song, "Optimal home energy management system with mixed types of loads," *CSEE J. Power Energy Syst.*, vol. 1, no. 4, pp. 29–37, Dec. 2015.
- [13] K. Murari and N. P. Padhy, "A network topology based approach for load flow solution of AC-DC distribution system with distributed generations," *IEEE Trans. Ind. Inform.*, vol. 15, no. 3, pp. 1508–1520, Mar. 2019.
- [14] K. Murari and N. P. Padhy, "An efficient load flow algorithm for AC-DC distribution systems," *Elect. Power Compon. Syst.*, vol. 46, no. 8, pp. 919–937, 2018.
- [15] D. J. Tylavsky and F. C. Trutt, "The Newton-Raphson load flow applied to AC/DC systems with commutation impedance," *IEEE Trans. Ind. Appl.*, vol. 19, no. 6, pp. 940–948, Nov./Dec. 1983.
- [16] H. M. A. Ahmed, A. B. Eltantawy, and M. M. A. Salama, "A generalized approach to the load flow analysis of AC-DC hybrid distribution systems," *IEEE Trans. Power Syst.*, vol. 33, no. 2, pp. 2117–2127, Mar. 2018.
- [17] K. Murari and N. P. Padhy, "Framework for assessing the economic impacts of AC-DC distribution network on the consumers," in *Proc. IEEE 59th Annu. Int. Sci. Conf. Power Elect. Eng. Riga Tech. Univ.*, 2018, pp. 1–5.
- [18] H. M. A. Ahmed, A. B. Eltantawy, and M. M. A. Salama, "A planning approach for the network configuration of AC-DC hybrid distribution systems," *IEEE Trans. Smart Grid*, vol. 9, no. 3, pp. 2203–2213, May 2018.

- [19] A. Ghadiri, M. R. Haghifam, and S. M. M. Larimi, "Comprehensive approach for hybrid AC/DC distribution network planning using genetic algorithm," *IET Gener. Transmiss. Distrib.*, vol. 11, no. 16, pp. 3892–3902, 2017.
- [20] S. Gao, H. Jia, and C. Marnay, "Techno-economic evaluation of mixed AC and DC power distribution network for integrating large-scale photovoltaic power generation," *IEEE Access*, vol. 7, pp. 105019–105029, 2019.
- [21] L. Zhang, Y. Chen, C. Shen, W. Tang, J. Liang, and B. Xu, "Optimal configuration of hybrid AC/DC urban distribution networks for high penetration renewable energy," *IET Gener. Transmiss. Distrib.*, vol. 12, no. 20, pp. 4499–4506, 2018.
- [22] C. Qi *et al.*, "A decentralized optimal operation of AC/DC hybrid distribution grids," *IEEE Trans. Smart Grid*, vol. 9, no. 6, pp. 6095–6105, Nov. 2018.
- [23] P. T. Baboli, M. Shahparasti, M. P. Moghaddam, M. R. Haghifam, and M. Mohamadian, "Energy management and operation modelling of hybrid AC–DC microgrid," *IET Gener. Transmiss. Distrib.*, vol. 8, no. 10, pp. 1700–1711, 2014.
- [24] A. A. Eajal, M. F. Shaaban, K. Ponnambalam, and E. F. El-Saadany, "Stochastic centralized dispatch scheme for AC/DC hybrid smart distribution systems," *IEEE Trans. Sustain. Energy*, vol. 7, no. 3, pp. 1046–1059, Jul. 2016.
- [25] Y. Fu, Z. Zhang, Z. Li, and Y. Mi, "Energy management for hybrid AC/DC distribution system with microgrid clusters using non-cooperative game theory and robust optimization," *IEEE Trans. Smart Grid*, vol. 11, no. 2, pp. 1510–1525, Mar. 2020.
- [26] H. M. A. Ahmed and M. M. A. Salama, "Energy management of AC–DC hybrid distribution systems considering network reconfiguration," *IEEE Trans. Power Syst.*, vol. 34, no. 6, pp. 4583–4594, Nov. 2019.
- [27] H. Gao, J. Wang, Y. Liu, L. Wang, and J. Liu, "An improved ADMM-Based distributed optimal operation model of AC/DC hybrid distribution network considering wind power uncertainties," *IEEE Syst. J.*, to be published, doi: [10.1109/JSYST.2020.2994336](https://doi.org/10.1109/JSYST.2020.2994336).
- [28] Q. Xu, T. Zhao, Y. Xu, Z. Xu, P. Wang, and F. Blaabjerg, "A distributed and robust energy management system for networked hybrid AC/DC microgrids," *IEEE Trans. Smart Grid*, vol. 11, no. 4, pp. 3496–3508, Jul. 2020.
- [29] F. Qiao and J. Ma, "Voltage/Var control for hybrid distribution networks using decomposition-based multiobjective evolutionary algorithm," *IEEE Access*, vol. 8, pp. 12015–12025, Jan. 2020.
- [30] F. Qiao and J. Ma, "Coordinated voltage/var control in a hybrid AC/DC distribution network," *IET Gener. Transmiss. Distrib.*, vol. 14, no. 11, pp. 2129–2137, 2020.
- [31] H. Lotfi and A. Khodaei, "Hybrid AC/DC microgrid planning," *Energy*, vol. 118, pp. 37–46, 2017.
- [32] Q. Geng *et al.*, "Optimal operation of AC–DC distribution network with multi park integrated energy subnetworks considering flexibility," *IET Renewable Power Gener.*, vol. 14, no. 6, pp. 1004–1019, 2020.
- [33] S. Paul, A. Sharma, and N. P. Padhy, "Optimal operation of a converter governed AC/DC hybrid distribution network with DERs," in *Proc. IEEE Int. Conf. Power Electron., Smart Grid Renewable Energy*, 2020, pp. 1–6.
- [34] S. Singh and S. P. Singh, "Energy saving estimation in distribution network with smart grid-enabled CVR and solar PV inverter," *IET Gener. Transmiss. Distrib.*, vol. 12, no. 6, pp. 1346–1358, 2018.
- [35] W. Shi, N. Li, X. Xie, C. C. Chu, and R. Gadh, "Optimal residential demand response in distribution networks," *IEEE J. Sel. Areas Commun.*, vol. 32, no. 7, pp. 1441–1450, Jul. 2014.
- [36] M. H. Hossan and B. Chowdhury, "Integrated CVR and demand response framework for advanced distribution management systems," *IEEE Trans. Sustain. Energy*, vol. 11, no. 1, pp. 534–544, Jan. 2020.
- [37] T. Xu and W. Wu, "Accelerated ADMM-based fully distributed inverter-based volt/var control strategy for active distribution networks," *IEEE Trans. Ind. Inform.*, vol. 16, no. 12, pp. 7532–7543, Dec. 2020.
- [38] H. Fan, C. K. Zhang, L. Jiang, C. Mao, and D. Wang, "ADMM-based multi-period optimal power flow considering plug-in electric vehicles charging," *IEEE Trans. Power Syst.*, vol. 33, no. 4, pp. 3886–3897, Jul. 2018.
- [39] N. Mohan, T. M. Undeland, and W. P. Robbins, *Power Electronics*. Hoboken, NJ, USA: Wiley, 2002.
- [40] R. T. Rockafellar and S. Uryasev, "Optimization of conditional value-at-risk," *J. Risk*, vol. 2, pp. 21–41, 1997.
- [41] H. P. Hong, "An efficient point estimate method for probabilistic analysis," *Rel. Eng. Syst. Saf.*, vol. 59, no. 3, pp. 261–267, 1998.
- [42] G. P. McCormick, "Computability of global solutions to factorable non-convex programs: Part-I—Convex underestimating problems," *Math. Program.*, vol. 10, no. 1, pp. 147–175, 1976.
- [43] S. R. Shukla, S. Paudyal, and M. R. Almassalkhi, "Efficient distribution system optimal power flow with discrete control of load tap changers," *IEEE Trans. Power Syst.*, vol. 34, no. 4, pp. 2970–2979, Jul. 2019.
- [44] S. Satsangi and G. B. Kumbhar, "Effect of load models on scheduling of VVC devices in a distribution network," *IET Gener. Transmiss. Distrib.*, vol. 12, no. 17, pp. 3862–3870, 2018.
- [45] M. Diaz-Aguiló *et al.*, "Field-Validated load model for the analysis of CVR in distribution secondary networks: Energy conservation," *IEEE Trans. Power Del.*, vol. 28, no. 4, pp. 2428–2436, Oct. 2013.
- [46] D. Han, J. Jian, and L. Yang, "Outer approximation and outer-inner approximation approaches for unit-commitment problem," *IEEE Trans. Power Syst.*, vol. 29, no. 2, pp. 505–513, Mar. 2014.
- [47] J. Lai, X. Lu, and F. Wang, "Bi-level information-aware distributed resilient control for heterogeneous microgrid cluster," *IEEE Trans. Ind. Appl.*, vol. 57, no. 3, pp. 2014–2022, May/Jun. 2021.
- [48] J. Lai and X. Lu, "Nonlinear mean-square power sharing control for AC microgrids under distributed event detection," *IEEE Trans. Ind. Inform.*, vol. 17, no. 1, pp. 219–229, Jan. 2021.



**Subho Paul** (Member, IEEE) received the B.Tech. degree in electrical engineering from the West Bengal University of Technology, Kolkata, India, in 2013, and the M.E. degree in electrical engineering with power system specialization from Jadavpur University, Kolkata, India, in 2016. He is currently working toward the Ph.D. degree in electrical engineering at the Department of Electrical Engineering, Indian Institute of Technology Roorkee, Roorkee, India.

His research interests include power system optimization, demand response analysis, power system analysis, storage applications in smart grids, and application of deep learning techniques in power system.

Mr. Paul was the recipient of the University Gold Medal for standing first in order of merit in the M.E. degree from Jadavpur University, Kolkata, India, in 2016. He was also the recipient of the Best Paper Award for the session Distribution System Analysis at International Conference on Power Systems, Jaipur, India, in 2019.



**Abhimanyu Sharma** received the B.Tech. degree in electrical engineering from the YMCA University of Science and Technology, Faridabad, India, in 2015, and the M.Tech. degree in power and energy system engineering from the National Institute of Technology, Silchar, India, in 2018. He is currently working toward the Ph.D. degree in electrical engineering at the Department of Electrical Engineering, Indian Institute of Technology Roorkee, Roorkee, India.

His research interests include power system analysis and optimization, demand response analysis, HEMS, and storage application in smart grid.

Mr. Sharma was the recipient of the University Topper's Medal for standing first in merit at the M.Tech. degree in power and energy system engineering at NIT Silchar.



**Narayana Prasad Padhy** (Senior Member, IEEE) received the Ph.D. degree in power systems engineering from Anna University, Chennai, India, in 1997.

He is working as a Professor (HAG) and 92 Batch Chair Professor with the Department of Electrical Engineering, Indian Institute of Technology (IIT) Roorkee, Roorkee, India. Earlier, he has served as a Dean of Academic Affairs, Institute, and NEEPCO Chair Professor with IIT Roorkee. He is the National Lead of many national and international projects such as DSIRES, ID-EDGE, and HEAPD. He is also part of other international projects, namely Indo-US UI-ASSIST, and Indo-U.K. ZED-I. He has authored/coauthored more than 150 research articles in reputed international journals and conference proceedings. His research interests include power system analysis, demand side management, energy market, network pricing, ac–dc smart grid, and application of machine learning techniques in power systems.

Prof. Padhy is a Fellow of the Indian National Academy of Engineers, Fellow Institution of Electronics and Telecommunication Engineers, India, Fellow Institution of Engineering and Technology, and Fellow of Institution of Engineers and India. He was the recipient of the IEEE PES Outstanding Engineers Award 2018, Boycecast Fellowship and the Humboldt Experienced research Fellowship in the year 2005 and 2009, respectively.